

Thermal diffusion of sine-Gordon solitons

Niurka R. Quintero¹, Angel Sánchez¹, and Franz G. Mertens²

¹ Grupo Interdisciplinar de Sistemas Complicados (GISC), Departamento de Matemáticas, Universidad Carlos III de Madrid, Edificio Sabatini, Avenida de la Universidad 30, E-28911 Leganés, Madrid, Spain
e-mail: kinter@math.uc3m.es, anxo@math.uc3m.es

² Physikalisches Institut, Universität Bayreuth, D-95440 Bayreuth, Germany
e-mail: franz.mertens@theo.phy.uni-bayreuth.de

Received: February 7, 2020/ Revised version:

Abstract. We analyze the diffusive motion of kink solitons governed by the thermal sine-Gordon equation. We analytically calculate the correlation function of the position of the kink center as well as the diffusion coefficient, both up to second-order in temperature. We find that the kink behavior is very similar to that obtained in the overdamped limit: There is a quadratic dependence on temperature in the diffusion coefficient that comes from the interaction among the kink and phonons, and the average value of the wave function increases with \sqrt{t} due to the variance of the centers of individual realizations and not due to kink distortions. These analytical results are fully confirmed by numerical simulations.

PACS. 05.40.-a Fluctuation phenomena, random processes, noise and Brownian motion – 05.45.-a Non-linear dynamics and nonlinear dynamical systems – 74.50.+r Proximity effects, weak links, tunneling phenomena, and Josephson effects – 85.25.Cp Josephson devices

1 Introduction

As a key subject within nonlinear science, the dynamics of emergent, coherent structures (solitons, vortices, etc) has been a research topic that has attracted very much attention in the past quarter century [1]. One question, extensively investigated in the literature [2,3,4,5,6,7] is the following: Is, and if so, how is the motion and the shape of those excitations modified by the presence of small perturbations? Indeed, when applied to physical situations of interest, nonlinear models must incorporate additional terms, such as damping, constant or periodic external forces, or noise, to name a few. Among those, stochastic perturbations are very much of interest in view of their highly non trivial effects on nonlinear systems [8], and a great deal of work has been devoted to them [2,4,5]. In particular, of the very many nonlinear models applied to physical problems, the sine-Gordon (sG) equation has been considered in much detail in this context, as it applies to, e.g., propagation of ultra-short optical pulses in resonant laser media [9], a unitary theory of elementary particles [10,11,12,13], propagation of magnetic flux in Josephson junctions [14], transmission of ferromagnetic waves [15], epitaxial growth of thin films [16,17,18], motion of dislocations in crystals [19,20], flux-line unlocking in type II superconductors [21], or DNA dynamics [22,23,24], situations in which noise (of different origins) can play, and often does, a crucial role. As an example, let us mention the recent work on long Josephson junctions reported in [25], where the authors calculated the escape

rate from the zero-voltage state induced by thermal fluctuations, obtaining very satisfactory results compared with the experimental ones.

Specifically, this work is devoted to the study of the diffusive dynamics of sG kink solitons subjected to a thermal bath, as given by the stochastically perturbed, damped sG equation

$$\phi_{tt} - \phi_{xx} + \sin(\phi) = -\alpha\phi_t + f(x, t, \phi, \dots), \quad (1)$$

where $-\alpha\phi_t$ is a damping term with a dissipation coefficient α , and $f(x, t, \phi, \dots)$ is a thermal (gaussian) noise term fulfilling

$$\begin{aligned} f(x, t, \phi, \dots) &= \sqrt{D} \eta(x, t), \quad \langle \eta(x, t) \rangle = 0, \\ \langle \eta(x, t) \eta(x', t') \rangle &= \delta(x - x') \delta(t - t'), \end{aligned} \quad (2)$$

where \sqrt{D} is related to temperature through the fluctuation-dissipation theorem $D = 2\alpha k_b T$, k_b being the Boltzmann constant and T the temperature.

To our knowledge, the first results on problems directly related to the one we deal with here were obtained by Joergensen *et al.* [26], who performed experiments on Josephson junctions and presented a derivation of the diffusion constant for kinks. Subsequently, Kaup and Osman [27] studied, in a more rigorous way, the motion of damped sG kinks, driven by a constant force, in the presence of thermal fluctuations by using a singular perturbation expansion. They analyzed the temperature effect

on the mean velocity of the kink and also the changes in the shape of the kink. In addition, they calculated the diffusion coefficient of the kink up to first-order in temperature and the energy values corresponding to the translational ($E_T = k_b T/2$) and radiational ($E_R = k_b T$) modes. These values of the energy have been also obtained by Marchesoni [28], who applied the McLaughlin and Scott approach [29] to investigate kink motion under thermal fluctuations (see [2,3,5] for reviews).

For the sake of completeness, let us mention work done along a different line, namely that devoted to the diffusive motion of the kink in equilibrium with phonons in *isolated sG systems* (possibly perturbed) [6,30,31,32]. In this case, the kink diffusive motion is characterized by two diffusion coefficients. The first one of them is proportional to T^2 and is related to the anomalous diffusion, that arises from the phase shifts of kinks colliding with phonons and takes place on a short time scale in which the collision among kink and wave packet is elastic; the kink retains the same velocity after the collision (non-dissipative diffusion) and suffers only a spatial shift. However, for large times and in slightly perturbed sG systems, this interaction is nonlinear and becomes inelastic and the velocity of the kink changes after the collisions [33]. This diffusive regime is called viscous and has a diffusion coefficient proportional to T^{-1} . The diffusion of the kink when the low energy excitations are represented by breathers has also been studied, and in [34] it has been demonstrated that both descriptions (breathers or phonons) are equivalent and give rise to the same diffusion coefficient in the anomalous regime.

In any event, we want to stress that, although in this type of diffusion problem there are many open questions [33], we will concern ourselves with the other kind of diffusion problem, in which the phonons appear as a consequence of *an external heat bath*, represented by white noise correlated in space and in time and the damping is included explicitly *à la* Langevin. The main aim of this work is to extend a previous study of ours about the overdamped limit of sine-Gordon kink diffusion [35] to the more physical and general case of the underdamped dynamics (i.e., with finite dissipation coefficient). As we will see below, the general perturbative approach [13] we resorted to in the overdamped case can also be applied, albeit with more difficulties, to the underdamped problem. The corresponding theoretical analysis is presented in Sec. 2, where we obtain explicit expressions for the long-time diffusive dynamics of kinks up to second-order in temperature, thus going beyond the currently available knowledge. The accuracy and importance of the new terms is assessed by numerical simulations in Sec. 3: we will see there that the quadratic corrections are in good agreement with the simulations and, most importantly, that they must be taken into account even for not so large temperatures. Finally, in the conclusions we summarize the main results of this work, comparing the underdamped and overdamped dynamics of the sG equation and discussing other related questions.

2 Analytical results

We begin by briefly reviewing the basic results we need for our analytical approach. We will concern ourselves with the perturbation effect on the kink solutions of the unperturbed sG equation, whose static form is

$$\phi_0(x, t) = 4 \arctan[\exp(x)]. \quad (3)$$

Small perturbations over this equation can be treated by calculating the spectrum of linear excitations around the kink solution [36]: To this end, we write

$$\phi(x, t) = \phi_0(x) + \psi(x, t), \quad \psi(x, t) \ll \phi_0(x), \quad (4)$$

substitute in (1) (with $\alpha = D = 0$) and linearize around $\phi_0(x)$, arriving at the following equation for $\psi(x, t)$:

$$\psi_{tt} = \psi_{xx} - \left[1 - \frac{2}{\cosh^2(x)} \right] \psi. \quad (5)$$

Then, assuming that the solution of (5) has the form

$$\psi(x, t) = f(x) \exp(i\omega t) \quad (6)$$

we find the eigenvalue problem for $f(x)$,

$$-\frac{\partial^2 f}{\partial x^2} + \left[1 - \frac{2}{\cosh^2(x)} \right] f = \omega^2 f. \quad (7)$$

This equation admits the following eigenfunctions with their respective eigenvalues

$$f_T(x) = \frac{2}{\cosh(x)}, \quad \omega_T^2 = 0, \quad (8)$$

$$f_k(x) = \frac{\exp(ikx)}{\sqrt{2\pi}} \frac{[k + i\tanh(x)]}{\omega_k}, \quad \omega_k^2 = 1 + k^2, \quad (9)$$

which represent, respectively, the translation (Goldstone) mode and the radiation modes. Importantly, the functions $f_T(x)$ and $f_k(x)$ form a complete set with the orthogonality relations

$$\int_{-\infty}^{+\infty} f_T^2(x) dx = 8, \quad (10)$$

$$\int_{-\infty}^{+\infty} f_T(x) f_k(x) dx = 0, \quad (11)$$

$$\int_{-\infty}^{+\infty} f_k(x) f_{k'}^*(x) dx = \delta(k - k'). \quad (12)$$

We can now proceed with our problem: In order to tackle Eq. (1), with noise as given in (2), we use the same *Ansatz* proposed for the overdamped case in [35] (or for the general Klein-Gordon system in [13]): We assume that the solution of Eq. (1) is

$$\phi(x, t) = \phi_0[x - X(t)] + \int_{-\infty}^{+\infty} dk A_k(t) f_k[x - X(t)], \quad (13)$$

where $X(t)$ is the kink position. We now insert (13) in (1) and use the orthogonality of f_k and f_T [36], obtaining the following system of differential equation for $X(t)$ and $A_k(t)$:

$$\begin{aligned}
\ddot{X}(t) + \alpha \dot{X}(t) = & -\frac{\alpha}{8} \dot{X}(t) \int_{-\infty}^{+\infty} dk A_k(t) I_1(k) - \frac{1}{16} \int_{-\infty}^{+\infty} dk \int_{-\infty}^{+\infty} dk' A_k(t) A_{k'}(t) R_3(k, k') + \\
& + \frac{\sqrt{D}}{8} \int_{-\infty}^{+\infty} f_T[x - X(t)] \eta(x, t) dx - \\
& - \frac{1}{48} \int_{-\infty}^{+\infty} dk \int_{-\infty}^{+\infty} dk_1 \int_{-\infty}^{+\infty} dk_2 A_k(t) A_{k_1}(t) A_{k_2}(t) R_6(k, k_1, k_2) - \\
& - \frac{\dot{X}(t)}{4} \int_{-\infty}^{+\infty} dk \frac{\partial A_k}{\partial t} I_1(k) - \frac{\ddot{X}(t)}{8} \int_{-\infty}^{+\infty} dk A_k(t) I_1(k) + \\
& + \frac{\dot{X}^2(t)}{8} \int_{-\infty}^{+\infty} dk \frac{\partial A_k}{\partial t} I_2(k),
\end{aligned} \tag{14}$$

$$\begin{aligned}
\frac{\partial^2 A_k}{\partial t^2} + \alpha \frac{\partial A_k}{\partial t} + \omega_k^2 A_k(t) = & \alpha \dot{X}(t) \int_{-\infty}^{+\infty} dk' A_{k'}(t) I_3(k', k) + \\
& + \frac{1}{2} \int_{-\infty}^{+\infty} dk \int_{-\infty}^{+\infty} dk' A_k(t) A_{k'}(t) R_4(k, k') - \\
& - \sqrt{D} \int_{-\infty}^{+\infty} f_k^*[x - X(t)] \eta(x, t) dx + \\
& + \frac{1}{6} \int_{-\infty}^{+\infty} dk' \int_{-\infty}^{+\infty} dk_1 \int_{-\infty}^{+\infty} dk_2 A_{k'}(t) A_{k_1}(t) A_{k_2}(t) R_7(k', k, k_1, k_2) + \\
& + 2\dot{X}(t) \int_{-\infty}^{+\infty} dk' \frac{\partial A_{k'}}{\partial t} I_3(k', k) + \\
& + \ddot{X}(t) \int_{-\infty}^{+\infty} dk' A_{k'}(t) I_3(k', k) + \dot{X}^2(t) I_1(k),
\end{aligned} \tag{15}$$

where

$$\begin{aligned}
I_1(k) &= \int_{-\infty}^{+\infty} \frac{\partial f_k}{\partial \theta} f_T(\theta) d\theta = \frac{i\pi\omega_k}{\sqrt{2\pi} \cosh\left(\frac{\pi k}{2}\right)}, \\
I_2(k) &= \int_{-\infty}^{+\infty} \frac{\partial^2 f_k}{\partial \theta^2} f_T(\theta) d\theta, \\
R_3(k, k') &= \int_{-\infty}^{+\infty} f_T(\theta) \frac{\partial f_T}{\partial \theta} f_k(\theta) f_{k'}^*(\theta) d\theta = -\frac{i(\omega_k^2 - \omega_{k'}^2)^2}{4\omega_k \omega_{k'} \sinh\left(\frac{\pi \Delta k}{2}\right)}, \quad \Delta k = k' - k, \\
I_3(k, k') &= \int_{-\infty}^{+\infty} \frac{\partial f_k}{\partial \theta} f_{k'}^*(\theta) d\theta, \\
R_4(k, k') &= \int_{-\infty}^{+\infty} [f_{k'}^*(\theta)]^2 \frac{\partial f_T}{\partial \theta} f_k(\theta) d\theta, \quad R_4(k, k) = \frac{3i\omega_k}{8\sqrt{2\pi} \cosh\left(\frac{\pi k}{2}\right)}, \\
R_6(k, k_1, k_2) &= \int_{-\infty}^{+\infty} \frac{\partial^2 f_T}{\partial \theta^2} f_k(\theta) f_{k_1}^*(\theta) f_{k_2}(\theta) d\theta, \\
R_7(k, k', k_1, k_2) &= \int_{-\infty}^{+\infty} \cos(\phi_0) f_{k'}^*(\theta) f_k(\theta) f_{k_1}^*(\theta) f_{k_2}(\theta) d\theta.
\end{aligned} \tag{16}$$

It goes without saying that these equations can not be solved. Therefore, in order to extract information from them, we resort to a perturbative approach assuming the noise term is small, or equivalently, that the temperature and the dissipation are not too large (this is not a serious restriction since our single-kink approach does not apply to high temperatures, when kink-antikink pairs are thermally generated [37]). We then expand $X(t)$ and $A_k(t)$ in powers

of \sqrt{D} , i.e., $X(t) = \sum_{n=1}^{\infty} (\sqrt{D})^n X_n(t)$ and $A_k(t) = \sum_{n=1}^{\infty} (\sqrt{D})^n A_k^n(t)$, since when $\sqrt{D} = 0$ and $\alpha = 0$ we recover the static kink solution (in this case initially centered at the origin) of the sG equation. By substituting these expansions in (14) and (15) we find a set of linear equations for the coefficients of these series. The first members of this hierarchy correspond to order $O(\sqrt{D})$:

$$\ddot{X}_1(t) + \alpha \dot{X}_1(t) = \frac{1}{8} \int_{-\infty}^{+\infty} f_T[x - X(t)] \eta(x, t) dx \equiv \epsilon_1(t), \quad (17)$$

from where we obtain the statistical properties of $\epsilon_1(t)$,

$$\langle \epsilon_1(t) \rangle = 0, \quad \langle \epsilon_1(t) \epsilon_1(t') \rangle = \frac{1}{8} \delta(t - t'), \quad (18)$$

and

$$\frac{\partial^2 A_k^1}{\partial t^2}(t) + \alpha \frac{\partial A_k^1}{\partial t}(t) + \omega_k^2 A_k^1(t) = \int_{-\infty}^{+\infty} f_k^*[x - X(t)] \eta(x, t) dx \equiv \xi_k(t), \quad (19)$$

which in turn leads to

$$\langle \xi_k(t) \rangle = 0, \quad \langle \xi_k(t) \xi_{k'}(t') \rangle = \delta(t - t') \delta(k - k'). \quad (20)$$

Equations (17)–(20) have been obtained in [38] by using a similar, but more restrictive perturbative approach. By integrating these two equations we obtain the first-order terms, $X_1(t)$ and A_k^1 :

$$\begin{aligned} X_1(t) &= \int_0^t e^{-\alpha t'} \int_0^{t'} e^{\alpha \tau} \epsilon_1(\tau) d\tau dt', \quad A_k^1(t) = e^{-\frac{\alpha t}{2}} \{C_1(t) \sin \omega t + C_2(t) \cos \omega t\}, \\ C_1(t) &= \frac{1}{\omega} \int_0^t \xi_k(\tau) e^{\frac{\alpha \tau}{2}} \cos \omega \tau d\tau, \quad C_2(t) = -\frac{1}{\omega} \int_0^t \xi_k(\tau) e^{\frac{\alpha \tau}{2}} \sin \omega \tau d\tau, \end{aligned} \quad (21)$$

where $\omega^2 = \omega_k^2 - (\alpha^2/4)$. From these relations we can calculate the mean values and correlation functions up to first order in \sqrt{D} :

$$\begin{aligned} \langle X_1(t) \rangle &= 0, \quad \langle X(t) X(t') \rangle = D \langle X_1(t) X_1(t') \rangle = \frac{D}{16\alpha^3} \left[e^{-\alpha M} - e^{-\alpha |\Delta t|} + e^{-\alpha M - \alpha |\Delta t|} - \right. \\ &\quad \left. - e^{-\alpha(t+t')} + e^{-\alpha t} + e^{-\alpha t'} + 2(\alpha M - 1) \right], \end{aligned} \quad (22)$$

$$\langle \dot{X}_1(t) \rangle = 0, \quad \langle \dot{X}(t) \dot{X}(t') \rangle = D \langle \dot{X}_1(t) \dot{X}_1(t') \rangle = \frac{D}{16\alpha} \left[e^{-\alpha |\Delta t|} - e^{-\alpha(t+t')} \right], \quad (23)$$

$$\begin{aligned} \langle A_k^1(t) \rangle &= 0, \quad \langle A_k(t) A_k(t') \rangle = D \langle A_k^1(t) A_k^1(t') \rangle = \frac{D}{\omega^2} e^{-\alpha(t+t')/2} \left[\frac{e^{\alpha M} - 1}{2\alpha} \cos \omega \Delta t - \right. \\ &\quad - \frac{\alpha e^{\alpha M}}{8\omega_k^2} \cos \omega \Delta t - \frac{\omega e^{\alpha M}}{4\omega_k^2} \sin \omega |\Delta t| + \frac{\alpha}{8\omega_k^2} \cos \omega(t+t') - \\ &\quad \left. - \frac{\omega}{4\omega_k^2} \sin \omega(t+t') \right], \end{aligned} \quad (24)$$

where $\Delta t = t - t'$, and $M = \min(t, t')$. Of course, for $t' = t$ in Eq. (22) we recover the result in [27] for $\langle [X(t)]^2 \rangle$.

We now turn to the main point of our work, namely obtaining the next-order corrections for the position and the velocity of the center of the kink. This requires the calculation of the next two contributions to $X(t)$ as well as the second order in the radiation terms, which are:

$O(D)$

$$\ddot{X}_2(t) + \alpha \dot{X}_2(t) = \epsilon_2(t), \quad (25)$$

$$\begin{aligned}\epsilon_2(t) \equiv & -\frac{\epsilon_1(t)}{8} \int_{-\infty}^{+\infty} dk A_k^1(t) I_1(k) - \frac{\dot{X}_1(t)}{4} \int_{-\infty}^{+\infty} dk \frac{\partial A_k^1}{\partial t}(t) I_1(k) - \\ & - \frac{1}{16} \int_{-\infty}^{+\infty} dk' \int_{-\infty}^{+\infty} dk A_k^1(t) A_{k'}^1(t) R_3(k, k'),\end{aligned}\quad (26)$$

$$\begin{aligned}\frac{\partial^2 A_k^2}{\partial t^2}(t) + \alpha \frac{\partial A_k^2}{\partial t}(t) + \omega_k^2 A_k^2(t) = & \epsilon_1(t) \int_{-\infty}^{+\infty} dk' A_{k'}^1(t) I_3(k', k) + \\ & + \frac{1}{2} \int_{-\infty}^{+\infty} dk \int_{-\infty}^{+\infty} dk' A_k^1(t) A_{k'}^1(t) R_4(k, k') - \\ & - \dot{X}_1^2(t) I_1(k) + 2 \dot{X}_1(t) \int_{-\infty}^{+\infty} dk' \frac{\partial A_{k'}^1}{\partial t}(t) I_3(k', k);\end{aligned}\quad (27)$$

$O([\sqrt{D}]^3)$

$$\ddot{X}_3(t) + \alpha \dot{X}_3(t) = \epsilon_3(t), \quad (28)$$

$$\begin{aligned}\epsilon_3(t) \equiv & -\frac{\epsilon_1(t)}{8} \int_{-\infty}^{+\infty} dk A_k^2(t) I_1(k) - \frac{\epsilon_2(t)}{8} \int_{-\infty}^{+\infty} dk A_k^1(t) I_1(k) - \\ & - \frac{1}{16} \int_{-\infty}^{+\infty} dk \int_{-\infty}^{+\infty} dk' A_k^2(t) A_{k'}^1(t) R_3(k, k') - \\ & - \frac{1}{16} \int_{-\infty}^{+\infty} dk \int_{-\infty}^{+\infty} dk' A_k^1(t) A_{k'}^2(t) R_3(k, k') - \\ & - \frac{1}{48} \int_{-\infty}^{+\infty} dk \int_{-\infty}^{+\infty} dk_1 \int_{-\infty}^{+\infty} dk_2 A_k^1(t) A_{k_1}^1(t) A_{k_2}^1(t) R_6(k, k_1, k_2) + \\ & + \frac{\dot{X}_1^2(t)}{8} \int_{-\infty}^{+\infty} dk \frac{\partial A_k^1}{\partial t}(t) I_2(k) - \frac{\dot{X}_1(t)}{4} \int_{-\infty}^{+\infty} dk \frac{\partial A_k^2}{\partial t}(t) I_1(k) - \\ & - \frac{\dot{X}_2(t)}{4} \int_{-\infty}^{+\infty} dk \frac{\partial A_k^1}{\partial t}(t) I_1(k).\end{aligned}\quad (29)$$

Analogously to what we have done for the first-order corrections, from the solutions of Eqs. (25) and (28) we find that

$$\langle X_2(t) \rangle = 0, \quad \langle \dot{X}_2(t) \rangle = 0, \quad (30)$$

$$\langle X_3(t) \rangle = 0, \quad \langle \dot{X}_3(t) \rangle = 0. \quad (31)$$

As for higher moments, taking into account that the cross-correlation function of $X_1(t)$ and $X_3(t')$ is of the same order as $\langle X_2(t) X_2(t') \rangle$, and also that $\langle X_1(t) X_2(t') \rangle = 0$ we obtain that

$$\begin{aligned}\langle [X(t)]^2 \rangle = & D \langle [X_1(t)]^2 \rangle + \\ & + D^2 (\langle [X_2(t)]^2 \rangle + 2 \langle X_1(t) X_3(t) \rangle) + \dots,\end{aligned}\quad (32)$$

$$\begin{aligned}\langle [\dot{X}(t)]^2 \rangle = & D \langle [\dot{X}_1(t)]^2 \rangle + \\ & + D^2 (\langle [\dot{X}_2(t)]^2 \rangle + 2 \langle \dot{X}_1(t) \dot{X}_3(t) \rangle) + \dots\end{aligned}\quad (33)$$

The expressions for the functions $\langle [X_2(t)]^2 \rangle$, $\langle [\dot{X}_2(t)]^2 \rangle$, $\langle X_1(t) X_3(t) \rangle$, and $\langle \dot{X}_1(t) \dot{X}_3(t) \rangle$ can be obtained after a lengthy calculation, and are very cumbersome indeed. We therefore do not include them here. However, for large time ($t >> 1/\alpha$) these relations can be simplified, yielding, as $t \rightarrow \infty$

$$\langle [X(t)]^2 \rangle = \frac{k_b T t}{4\alpha} \left\{ 1 + \frac{k_b T}{32} \left(1 + \frac{9\sigma^2}{4} \right) \right\}, \quad (34)$$

$$\langle [\dot{X}(t)]^2 \rangle = \frac{k_b T}{8} \left\{ 1 + \frac{3k_b T}{128} \left(12 + \sigma^2 \right) \right\}, \quad (35)$$

with

$$\sigma = \int_{-\infty}^{+\infty} \frac{dk}{\omega_k \cosh \left(\frac{\pi k}{2} \right)} = 1.62386. \quad (36)$$

To complete the characterization of the kink diffusion, we can now compute in a straightforward way the average value of the wave function $\phi(x, t)$, defined as

$$\begin{aligned} \langle \phi(x, t) \rangle &= \langle \phi_0[x - \sqrt{D}X_1(t)] \rangle + O(D) = \\ &= \int_{-\infty}^{+\infty} dX_1 p(X_1) \phi_0[x - \sqrt{D}X_1(t)], \end{aligned} \quad (37)$$

where $p(X_1)$ is the probability distribution function for X_1 . To find explicitly this function we note that, if we rewrite Eq. (17) as a system of two differential equations,

$$\begin{aligned} \dot{X}_1 &= V, \\ \dot{V} &= -\alpha V + \epsilon_1(t), \end{aligned} \quad (38)$$

the last equation represents an Ornstein-Uhlenbeck process for the velocity, and its distribution function is given by

$$p(V) = \sqrt{\frac{1}{2\pi\langle V^2 \rangle}} \exp \left(-\frac{V^2}{2\langle V^2 \rangle} \right), \quad (39)$$

(see [39]). Subsequently, by integrating the first equation of (38), we obtain that $X_1 = \int_0^t V(\tau) d\tau$. Since V has a Gaussian distribution function, X_1 has also a Gaussian distribution function, given by (recall that $\langle X_1(t) \rangle = 0$)

$$p(X_1) = \sqrt{\frac{1}{2\pi\langle [X(t)]^2 \rangle}} \exp \left(-\frac{X_1^2}{2\langle [X(t)]^2 \rangle} \right), \quad (40)$$

where the first and second moments of X_1 were obtained before, see Eq. (22). With this result, the integral (37), can be evaluated numerically taking into account Eqs. (40) and (22). In the next section we will compare this result with the mean value of the wave function as obtained from simulations of the full partial differential equation (1).

3 Numerical simulations

In order to test the approximate theory developed in the previous section, we have simulated numerically Eq. (1)

by using the Heun method [40]. In our simulations we begin with a kink, initially at rest, with free boundary conditions. For the damping coefficient we choose $\alpha = 0.1$, which is not too small because from (34) we can see that $\langle [X(t)]^2 \rangle$ is proportional to $1/\alpha$. This means that if α is too small the kink can move in a much larger region, forcing us to increase the length of our simulated system in the simulations, already quite time consuming. Furthermore, the relation (34) is only valid for large times ($t \gg 1/\alpha$). Again, for too small α we would need to simulate our equation for very long times and, as $\langle [X(t)]^2 \rangle$ increases linearly with time [see Eq. (34)], the system length would once more have to be large. The other parameters are $\Delta x = 0.2$, $\Delta t = 0.001$ and the length of the system $L = 200$. We have calculated all average values over 1000 realizations up to a final time 400. It is important to point out that, this system being inertial, the accuracy of the averages is considerably less than for overdamped problems, this being the reason why we have to use such large ensembles of trajectories to obtain reasonably good results.

An important, nontrivial issue is the question as to how can we find the center of the kink. We solve this problem by finding all the discrete lattice points x_i and x_{i+1} such that $\phi_i \leq \pi$ and $\phi_{i+1} \geq \pi$ or vice versa, and then estimating the corresponding points \tilde{x}_i where $\phi = \pi$ by linear interpolation. Afterwards, among the n such points \tilde{x}_n , we choose to be the center of the kink the value $\tilde{x} = \tilde{x}_n$, which minimizes $\sum_{i=1}^{L/\Delta x} [\phi_i(t) - \phi_0(x - \tilde{x}_n, t)]^2$, i.e., the discrete version of the integral of the square of the difference of ϕ and ϕ_0 . It has to be realized that this involves an assumption, namely that individual realizations of the kink have a shape similar to that of the unperturbed kink. As can be seen from Fig. 1, where the individual realizations are compared with the initial condition (an exact kink), this is indeed the case and our procedure is truly sensible. Therefore, we are sure that this method to compute the kink center avoids the false centers, which can appear for higher temperatures due to fluctuations introducing a systematic difference between the numerical and the theoretical results (see [35]). With the procedure we have just summarized, that works even for relatively large temperatures, we believe we find a very accurate approximation to the actual center of the kink. We will come back to Fig. 1 below.

As an example of the comparison of the numerical simulations of Eq. (1) with the theoretical results obtained in the previous section and valid for large times, Fig. 2 shows the numerically computed variance of the center of the kink, $\langle [X(t)]^2 \rangle - \langle X(t) \rangle^2$, as well as the first- and second-order analytical expressions. The plot clearly evidences that the numerical variance asymptotically coincides with the second-order expression: Note that to compare the different curves one has to look at the *slopes* at times $t \gg 1/\alpha$ (in this case, $t \geq 100$, for instance, as $\alpha = 0.1$); the theoretical result is not valid at early times and therefore there is a bias between analytics and numerics coming from that. The small, irregular oscillations in the numerical curve arise from the difficulty in accurately computing averages in an underdamped system like this

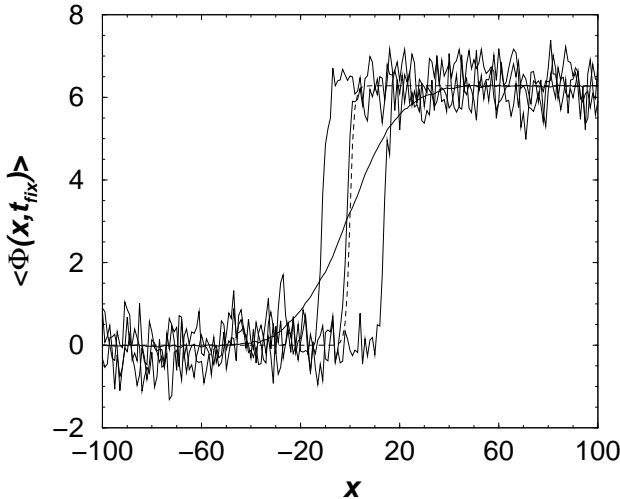


Fig. 1. Individual kink realizations compared with initial conditions and averages. Shown are three individual realizations at $t = 300$ with parameters $k_B T = 0.4$ and $\alpha = 0.1$ (thin solid lines), the initial condition given by a kink at rest (dashed line) and the mean value of ϕ at the same time obtained from averaging over 1000 realizations (thick solid line).

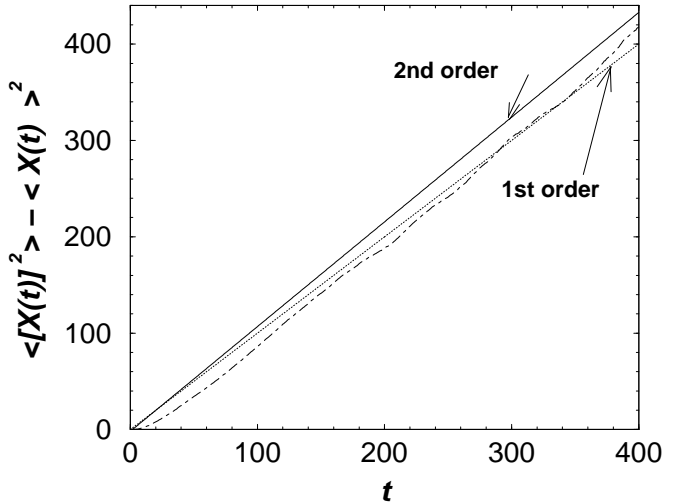


Fig. 2. Comparison of analytical and numerical results for the variance of the kink center, $\langle [X(t)]^2 \rangle - \langle X(t) \rangle^2$, for $k_B T = 0.4$. The dot-dashed line is the result of the numerical simulation of Eq. (1), whereas the dotted and the solid lines are the analytical results for the first- (dotted line) and second-order (solid line) expressions [Eqs. (22) and (34) with $t = t'$ respectively]. Only the slopes of the lines for $t >> 10$ have to be compared.

mentioned above; however, we believe that the present accuracy is enough to confirm the validity of our approach. We have observed the same agreement for other values of temperatures ($k_B T = 0.2, 0.6, 0.8$, not shown). In all cases, we have computed the diffusion coefficient for large times as the slope of the variance of $X(t)$ again for $t \geq 100$, the regime in which we expect our analytical approximation to be valid. Summarizing our results, these numerical values of the diffusion coefficient are plotted in Fig. 3 together with the theoretical results. It is clear that for large temperatures the quadratic behavior in $k_B T$ of the diffusion coefficient becomes important. For higher values of the temperature, such as $k_B T = 0.8$, the numerical value of the diffusion coefficient is not so close to the predicted one. This effect arises because of the large diffusivity of the kink in that range: Indeed, for this and higher temperatures the kink performs very long excursions away from the center, reaching the boundaries of the numerical integration interval; it is clear that when this occurs, the diffusion of the kink is not in free space anymore and hence those realizations spoil the quality of the averages. The way to solve this problem would be to resort to much larger numerical systems, but within our present computing capabilities this would necessitate a simultaneous decrease in the number of realizations in the average, leading again to poorer results. However, it is important to realize that this boundary effect leads to an *underestimation* of the diffusion coefficient (as the boundary prevents the kink from travelling as far as it should) and therefore the point in Fig. 3 for $k_B T = 0.8$ is a lower bound for the diffusion coefficient, with the actual one lying even closer to our second order prediction.

Finally, there is one last question that deserves discussion, namely that of the physical significance of the mean value of the wave function ϕ . In Fig. 1 we can clearly see that, whereas individual realizations of kinks look very similar to the unperturbed ones, the mean value of ϕ is a much wider excitation, not even close to the original kink. Figure 1 clearly shows that this does not mean that the width of individual kinks increases; indeed, much as we discussed regarding the overdamped problem [35], we have verified numerically that the mean wave function $\langle \phi(x, t_{fix}) \rangle$ increases due to the variance of the kink center of individual realizations, and hence it should not be interpreted as the typical deformation of the shape of kinks: Indeed, the widening of the mean value of ϕ arises from the contributions of the stochastically moving, but mostly undistorted kinks whose center positions have the distribution of a rigid, diffusing particle. To further check this interpretation, we can look at Fig. 4, where we have represented the mean value of the wave function for two fixed times $t_{fix} = 100, 300$, obtained from the numerical simulation of the full partial differential equation (1), for $k_B T = 0.6$ and $\alpha = 0.1$. The overimposed points, computed by using the Gaussian distribution function $p(X_1)$ [Eq. (40)] of the kink center $X(t) = \sqrt{D}X_1$ found in the last section, show the excellent agreement between our theory and the simulation. Of course, there is a small discrepancy that is likely to disappear if one would go to a next order calculation, but for the present purpose of understanding the mean wave function ϕ the first order calculation is enough. In addition, we have plotted the initial kink (at rest) in order to see that the mean value of the wave function increases with time.

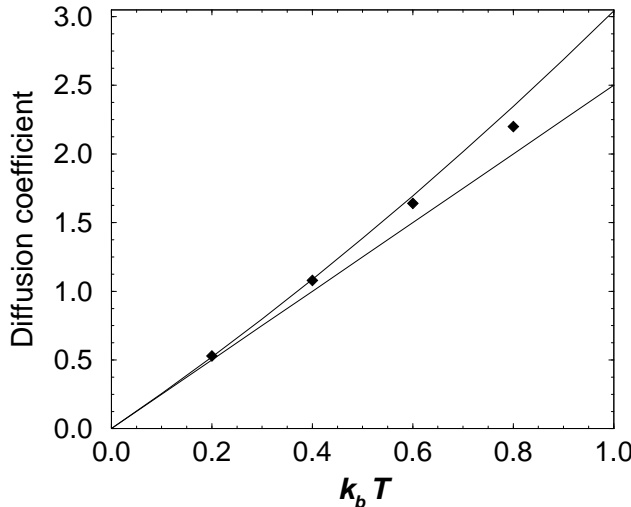


Fig. 3. Kink diffusion constant vs temperature. The solid lines represent the analytical diffusion coefficient up to first- (lower line) and second-order (upper line). Diamonds stand for numerical values of the kink center diffusion coefficient, obtained by numerical integration of Eq. (1).

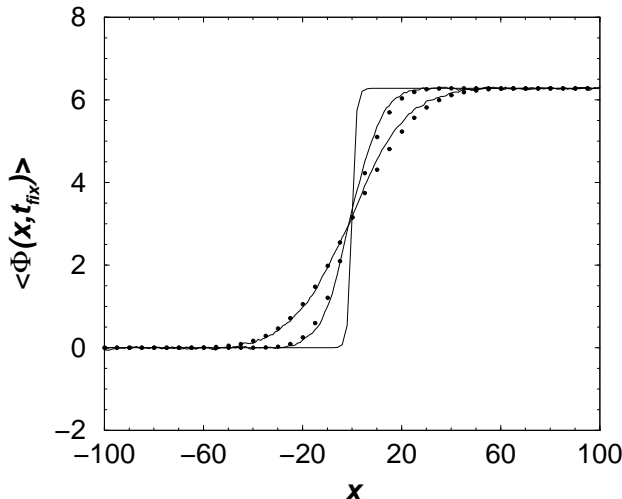


Fig. 4. Mean value of the wave function (solid line) for two fixed times, $t_{fix} = 100$ and $t_{fix} = 300$, with $k_b T = 0.6$, obtained from numerical simulations of Eq. (1) compared to the values of $\langle \phi(x, t) \rangle$ (points) obtained numerically from the integral in Eq. (37). The narrowest solid line is the initial data (kink initially at rest).

4 Discussion and conclusions

To summarize, in this work we have studied the diffusive dynamics of sine-Gordon kinks subjected to thermal fluctuations. We have analytically calculated expressions, valid up to second order in temperature, for the average position and variance of the kink center, as well as for the mean shape of the kink. We have numerically checked the validity of these results up to temperatures of the order

of $k_b T = 0.8$ (in dimensionless units, equivalent to about a 10% of the kink rest mass), already close to the temperature at which kink-antikink nucleation becomes a likely event. Therefore, our first conclusion is that the second-order theory developed here is the proper one, meaning it is accurate and higher order terms are negligible, to describe the thermal diffusion of sine-Gordon kinks in the single kink propagation regime. Interestingly, our calculation pinpoints the fact that the second-order correction in $k_b T$ comes from the interaction between kink and phonons. This implies that the physics behind this contribution is basically the same as for the case of anomalous diffusion in an isolated chain mentioned in the introduction [6, 30, 31, 32]. Note that we do not expect T^{-1} contributions in our analytical calculations, as they are carried out in a continuum sG equation [6] and, in any case, they would show up in simulations only for very low temperatures. Apart from that, it is also interesting to note that, according to Eq. (35), the second order term implies an increase of the energy carried by the kink beyond the $k_b T/2$ predicted by statistical mechanics (recall that the kink mass is 8 in our units). This can be interpreted in the following way: The kink is dressed by phonons which increase its mass. Thus, the kink energy would be $M(T) \cdot \dot{X}^2/2$, with a temperature dependent mass $M(T)$ whose expression can be easily found from Eq. (35). In order to confirm this interpretation, one could compute the energy carried by the phonons which dress the kink, but we believe that it is not necessary because, on the one hand, it would be a rather involved calculation (far beyond the scope of this work) and, on the other hand, we do not think that there is any other possible interpretation of this result.

A second relevant point of this study relates to the numerical simulation and center location procedures. As this is an underdamped (inertial) system, the thermal mobility of kinks is quite large, the larger the higher the temperature. Because of this, we have not been able to obtain very precise numerical averages at the top of the temperature range studied, since the lengths of the systems and the number of realizations required are very large and consequently time consuming. However, we believe that the results presented here are enough to verify our theory. This is reinforced by the very good agreement between analytics and numerics regarding the mean shape of the field, even for temperatures as large as $k_b T = 0.6$ (see Fig. 3), which shows that our approach indeed captures the physics of the diffusion process. In addition, we want to emphasize that, to our knowledge, we have designed a new algorithm to detect the kink center which gives very good results even for the highest temperatures studied, where previous researches, such as [35], had found problems arising from the many false centers detected.

Another important issue is the comparison of the present analysis to that in [35] for the overdamped problem. We have found that the diffusion coefficient given by (34) for the present case practically coincides with that obtained in [35] for the overdamped limit of the equation: the difference in the second order is approximately $0.06 k_b T$, i.e., very small compared to the magnitude of

the quadratic contribution itself. Furthermore, the width of the mean value of the wave function increases with time for the overdamped case [35] in the same manner as that reported here. Therefore, we can conclude that for large times the dynamic of the underdamped sG kinks is very similar to the overdamped case. This is an important point, because in principle one can expect similar results for other kink-bearing systems such as the ϕ^4 equation, for instance, whose overdamped diffusive dynamics is known (see [42] for the ϕ^4 case), thus avoiding the much more involved calculation of the underdamped case.

Finally, we want to mention the relevance of this work to experimental systems, such as long Josephson junctions. As has been shown in [25], the thermal sG equation (1) is a good description of the physics of in-line Josephson junctions (although different boundary conditions are needed in that case). The work in [25] compared the predictions from the sG model to experimentally measured escape rates from the zero voltage state. Therefore, it should be possible to design similar experiments in order to test our results and, specifically, the increased (quadratic) diffusivity of kinks at higher temperatures vs the linear behavior at lower ones. We hope that our theoretical work stimulates further experimental research in that direction.

Acknowledgement

We are grateful to A. R. Bishop for his comments and Esteban Moro for his suggestions. Work at GISC (Leganés) has been supported by CICYT (Spain) grant MAT95-0325 and DGES (Spain) grant PB96-0119. Travel between Bayreuth and Madrid is supported by “Acciones Integradas Hispano-Alemanas”, a joint program of DAAD (Az. 314-AI) and DGES. This research is part of a project supported by NATO grant CRG 971090.

References

1. A. C. Scott, *Nonlinear Science* (Oxford University Press, Oxford, 1999).
2. F. G. Bass, Yu. S. Kivshar, V. V. Konotop, and Yu. A. Sinitsyn, Phys. Rep. **157**, 63 (1988).
3. Yu. S. Kivshar and B. A. Malomed, Rev. Mod. Phys. **61**, 763 (1989).
4. A. Sánchez and L. Vázquez, Int. J. Mod. Phys. B, 2825 (1991).
5. V. V. Konotop and L. Vázquez, *Nonlinear random waves* (World Scientific, Singapore, 1994).
6. O. M. Braun and Yu. S. Kivshar, Phys. Rep. **306**, 1 (1998).
7. A. Sánchez and A. R. Bishop, SIAM Rev. **40**, 579, (1998).
8. J. García-Ojalvo and J. M. Sancho, *Noise in spatially extended systems* (Springer, New York, 1999).
9. G. L. Lamb, Rev. Mod. Phys. **43**, 99 (1971).
10. T. H. R. Skyrme, Proc. Roy. Soc. London **A247**, 260 (1958).
11. T. H. R. Skyrme, Proc. Roy. Soc. London **A262**, 237 (1961).
12. U. Enz, Phys. Rev. **131**, 1392 (1963).
13. R. Rajaraman, *Solitons and Instantons* (North-Holland Publishing Company, Amsterdam, 1982).
14. A. Barone and G. Paternó, *Physics and applications of the Josephson effect* (Wiley, New York, 1982).
15. E. Feldtkeller, Phys. Stat. Sol. **27**, 161 (1968).
16. J. D. Weeks and G. H. Gilmer, Adv. Chem. Phys. **40**, 157 (1979).
17. J. Krug and H. Spohn, Europhys. Lett. **8**, 219 (1989).
18. A. Sánchez, D. Cai, N. Grønbech-Jensen, A. R. Bishop, and Z. J. Wang, Phys. Rev. B **51**, 14664 (1995).
19. J. Frenkel and T. Kontorova, J. Phys. USSR, **1**, 137 (1939).
20. F. R. N. Nabarro, *Theory of crystal dislocations* (Dover, New York, 1987).
21. C. Cattuto and F. Marchesoni, Phys. Rev. Lett. **79**, 5070 (1997).
22. S. W. Englander, N. R. Kallenbach, A. J. Heeger, J. A. Krumhansl and S. Litwin, Proc. Natn. Acad. Sci. USA **77**, 7222 (1980).
23. M. Salerno, Phys. Rev. A **44**, 5292 (1991).
24. L. V. Yakushevich, Reviews of Biophysics **26**, 201 (1993).
25. M. G. Castellano, G. Torrioli, C. Cosmelli, A. Costantini, F. Chiarello, P. Carelli, G. Rotoli, M. Cirillo and R. L. Kautz, Phys. Rev. B **54**, 15417 (1996).
26. E. Joergensen, V. P. Koshelets, R. Monaco, J. Mygind, and M. R. Samuels, Phys. Rev. Lett. **49**, 1093 (1982).
27. D. J. Kaup and E. Osman, Phys. Rev. B **33**, 1762 (1986).
28. F. Marchesoni, Phys. Lett. A **115**, 29 (1986).
29. D. W. McLaughlin and A. C. Scott, Phys. Rev. A **18**, 1652 (1978).
30. Y. Wada and J. R. Schieffer, Phys. Rev. B **18**, 3897 (1978).
31. F. Marchesoni and C. R. Willis, Phys. Rev. A **36**, 4559 (1987).
32. F. Marchesoni and C. R. Willis, Europhys. Lett. **12**, 491 (1990).
33. Y. Wada, Prog. Theo. Phys. Suppl. **113**, 1 (1993).
34. N. Theodorakopoulos and E. W. Weller, Phys. Rev. B **38**, 2749 (1988).
35. N. R. Quintero, A. Sánchez and F. G. Mertens, Phys. Rev. E, **60**, 222 (1999).
36. M. B. Fogel, S. E. Trullinger, A. R. Bishop and J. A. Krumhansl, Phys. Rev. B **15**, 1578 (1977).
37. M. Büttiker and R. Landauer, in *Nonlinear phenomena at phase transitions and instabilities*, T. Riste, ed. (Plenum Publishing Corp., New York, 1982).
38. M. Salerno, E. Joergensen, and M. R. Samuels, Phys. Rev. B **30**, 2635 (1984).
39. W. Horsthemke and R. Lefever, *Noise-Induced Transitions* (Springer-Verlag Berlin 1984).
40. Stochastic effects in Physical Systems, M. San Miguel, and R. Toral, *Instabilities and Nonequilibrium Structures V*, edited by E. Tirapegui, W. Zeller. (Kluwer, Dordrecht, 1997).
41. W. H. Press, S. A. Teukolsky, W. T. Vetterling and B. P. Flannery, *Numerical Recipes in Fortran 2nd Edition* (Cambridge University Press, Cambridge, 1992).
42. J. Dziarmaga and W. Zakrzewski, Phys. Lett. A **251**, 85 (1999).